SANDIA REPORT

SAND2000-1049
Unlimited Release
Printed May 2000

Composite Resonator Surface Emitting Lasers

A. J. Fischer, K. D. Choquette, W. W. Chow, A. A. Allerman, and K. M. Geib

Prepared by
Sandia National Laboratories
Albuquerque, New Mexico 87185 and Livermore, California 94550

Sandia is a multiprogram laboratory operated by Sandia Corporation, a Lockheed Martin Company, for the United States Department of Energy under Contract DE-AC04-94AL85000.

Approved for public release; further dissemination unlimited.

Sandia National Laboratories

Issued by Sandia National Laboratories, operated for the United States Department of Energy by Sandia Corporation.

Available to DOE and DOE contractors from
Office of Scientific and Technical Information
P.O. Box 62
Oak Ridge, TN 37831

Prices available from (703) 605-6000
Web site: http://www.ntis.gov/ordering.htm

Available to the public from
National Technical Information Service
U.S. Department of Commerce
5285 Port Royal Rd
Springfield, VA 22161

SAND2000-1049
Unlimited Release
Printed May 2000

Composite Resonator Surface Emitting Lasers

A.J. Fischer, K.D. Choquette, W.W. Chow, A.A. Allerman, and K.M. Geib.
Center for Compound Semiconductor Science and Technology
Sandia National Laboratories
P.O. Box 5800
Albuquerque, NM 87185-0603

Abstract

We have developed electrically-injected coupled-resonator vertical-cavity lasers and have studied their novel properties. These monolithically grown coupled-cavity structures have been fabricated with either one active and one passive cavity or with two active cavities. All devices use a selectively oxidized current aperture in the lower cavity, while a proton implant was used in the active-active structures to confine current in the top active cavity. We have demonstrated optical modulation from active-passive devices where the modulation arises from dynamic changes in the coupling between the active and passive cavities. The laser intensity can be modulated by either forward or reverse biasing the passive cavity. We have also observed Q-switched pulses from active-passive devices with pulses as short as 150 ps. A rate equation approach is used to model the Q-switched operation yielding good agreement between the experimental and theoretical pulseshape. We have designed and demonstrated the operation of active-active devices which lase simultaneously at both longitudinal cavity resonances. Extremely large bistable regions have also been observed in the light-current curves for active-active coupled resonator devices. This bistability can be used for high contrast switching with contrast ratios as high as 100:1. Coupled-resonator vertical-cavity lasers have shown enhanced mode selectivity which has allowed devices to lase with fundamental-mode output powers as high as 5.2 mW.

Acknowledgments:

The authors are indebted to many researchers formerly and presently from Sandia, including B.E. Hammons, D. Serkland, G. R. Hadley, and J.J. Hindi.

This work was supported by the United States Department of Energy under Contract DE-AC04-94AL85000. Sandia is a multiprogram laboratory operated by Sandia Corporation for the United States Department of Energy.

COMPOSITE RESONATOR SURFACE EMITTING LASERS

Table of Contents

COMPOSITE RESONATOR SURFACE EMITTING LASERS

Table of Figures

1. Introduction

For many applications, the device performance of edge emitting semiconductor lasers can be significantly improved through the use of multiple section devices. For example, cleaved-coupled-cavity lasers have been shown to provide single longitudinal mode operation, wavelength tuning, high speed switching, as well as the generation of short pulses via mode-locking and Q-switching [1]. Using composite-resonators [2] within a vertical-cavity surface-emitting laser (VCSEL) opens up new possibilities due to the unique ability to: (i) tailor the coupling between the monolithic cavities; (ii) dynamically modify the cavity interaction; and (iii) incorporate passive or active resonators. Composite resonators can be utilized to influence the spectral and temporal properties within a vertical cavity laser. The goal of this research was to investigate the novel properties of coupled-resonator vertical-cavity lasers (CRVCLs) for both active-passive and active-active configurations.

For active-passive devices, one cavity contains an electrically-injected active region, while the other (passive) cavity contains only a bulk GaAs region. Current injection into the passive cavity produces no gain, but causes changes in the thermal and electronic properties of that cavity. This structure allowed us to separate effects arising from the two degenerate gain regions which are characteristic of the active-active devices. The active-passive structure was designed to be used as a modulator. Efficient modulation of the laser emission can be achieved by either forward or reverse biasing the passive cavity [3,4]. Under forward bias modulation, the CRVCL devices use a novel mechanism based on changes in cavity coupling to modulate the output intensity. Under reverse bias operation of the passive cavity, the modulation is caused by the Franz-Keldysh effect in the passive cavity. Furthermore, under reverse bias operation, Q-switched pulses have been observed [5]. The Q-switched operation is possible in this structure due to cavity coupling which allows large changes in the cavity Q with only very small changes in absorption. The ability to generate optical pulses from VCSELs is of great importance in the development of high speed optical data links, where very short pulses at high repetition rates are required in a small, economical package. These Q-switched pulses also have the potential to have much lower chirp than pulses produced via direct current modulation of a single VCSEL device.

Active-active devices have also been fabricated and have demonstrated many new and interesting properties. It is possible to design a CRVCL to lase simultaneously at both longitudinal cavity resonances. The separation between the longitudinal modes can be tailored for various applications by varying the reflectivity of the middle distributed Bragg reflector (DBR). As demonstrated below, it is also possible to switch between two widely separated wavelengths by modulating the injected current to one active region. Active-active devices can also exhibit bistable behavior in the light-current curve when one active region is properly biased [6]. There is much interest in demonstrating reliable bistable operation in VCSELs, especially in the form of compact two dimensional arrays, which would be promising laser sources for use in optoelectronic integrated circuits. As demonstrated below, the bistability in CRVCL devices can lead to high contrast switching at very low electrical switching powers. Active-active devices exhibit an enhanced transverse mode selectivity compared to a single VCSEL. We have achieved fundamental mode powers as high as 5.2 mW from the CRVCL devices studied here [7].

2. Device Structure

Figure 1 shows a schematic diagram of a typical active-active CRVCL structure. The coupled-resonator is composed of a bottom p-type distributed Bragg reflector (DBR) with 35 periods, a middle n-type DBR with 11.5 periods, and a top p-type DBR with 22 periods. The top and bottom one-wavelength cavities each contain five 8 nm GaAs quantum wells. The device was fabricated using a two-tier etch with two metal ring contacts on the top as well as a back side contact. Current can be independently injected into either cavity. In the bottom active cavity we employ selective oxidation of AlGaAs to form buried oxide layers for efficient electrical and optical confinement. A proton implant was used for current confinement in the top cavity. Devices were fabricated with and without the proton implant for comparison. The active-passive structures were fabricated with the same basic structure with the exception that the upper cavity was the passive cavity and consisted of a 1/2-λ layer of bulk GaAs and the quantum wells in the lower cavity were composed of InGaAs for emission at 980 nm.

Figure 2 shows the measured reflectance of a CRVCL structure. The coupling between the two cavities can be accurately controlled by changing the number of periods of the middle n-DBR. The inset of Fig. 2 shows the calculated cavity resonances as a function of periods in the middle DBR. The cavity resonances are determined by the transmission of the shared middle DBR. Our experimental separation of 14 nm for an 11.5 period DBR agrees well with the calculation. We have fabricated devices with middle DBRs from 7.5 mirror pair up to 15.5 mirror pair. Figure 3 shows the cavity resonance splitting for each of the devices fabricated in this study together with the calculated cavity splitting. Since devices operating at both 850 nm and 980 nm were fabricated, the splitting is normalized to the operating wavelength and $\Delta\lambda/\lambda$ was plotted. Results from several other research groups were also included for completeness [7,8]. Note that a resonance splitting as large as 30 nm is easily achievable. Since the splitting can be tailored by changing the middle mirror reflectivity, these devices will be useful as tunable multiple wavelength sources.

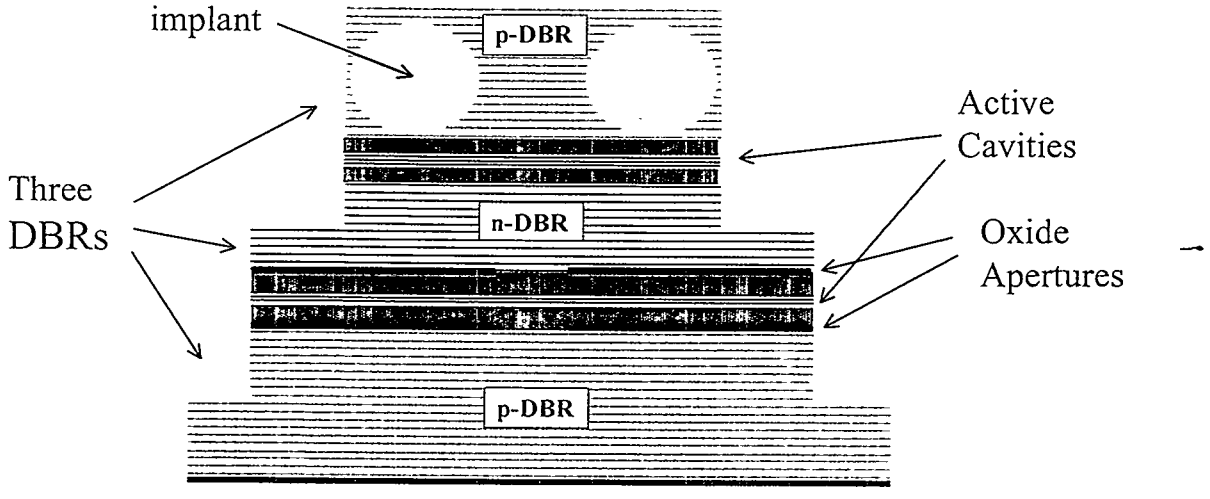

Figure 1. Schematic diagram of a coupled-resonator vertical-cavity laser (CRVCL).

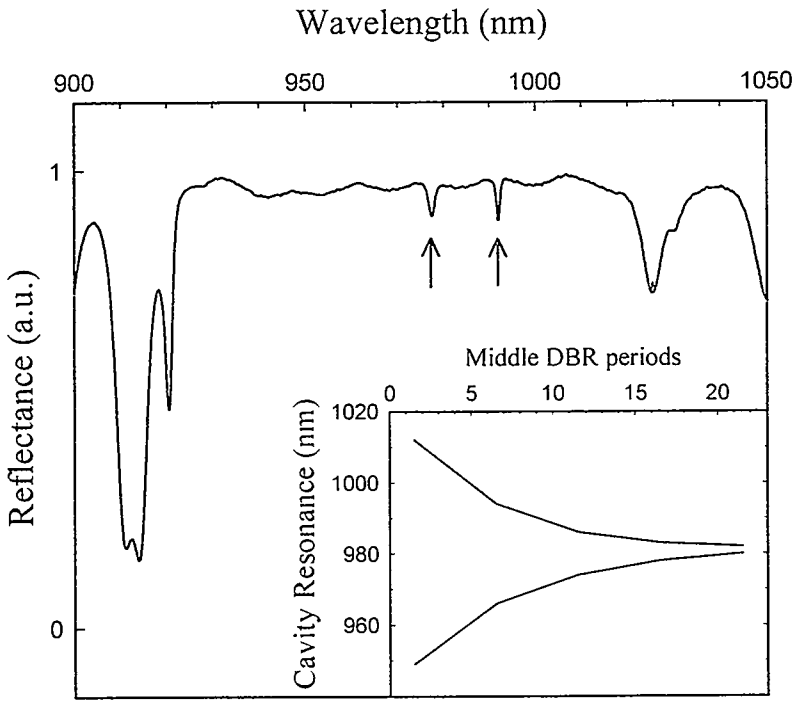

Figure 2. Reflection spectrum taken from a coupled-resonator vertical-cavity laser. The inset shows the resonance splitting as a function of number of middle mirror pairs

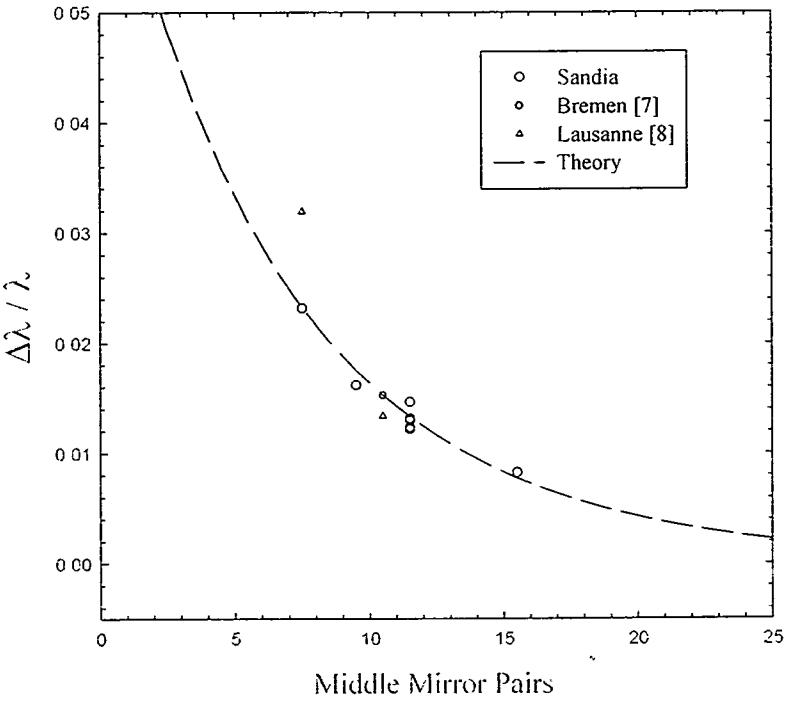

Figure 3. Normalized cavity resonance splitting plotted as a function of middle mirror pairs.

3. Active-Passive Devices

Although direct current modulation of a VCSEL is the most straight forward method of optical modulation, there are several inherent disadvantages. Direct current modulation where the injected current swings above and below the lasing threshold provides a large change in optical intensity for good contrast between the on and off states; however, the modulation speeds are limited and the wavelength will change due to carrier induced refractive index effects. This change in wavelength is undesirable for many applications. On the other hand, when the injection current supplied to a single VCSEL is modulated and the device remains above threshold, the modulation speed is fast, but the optical intensity contrast is low. By using a multiple section laser, it is possible to keep one section above the lasing threshold while using the other section as an optical modulator. This method can potentially provide high contrast switching with very low chirp. Our goal in fabricating active-passive CRVCL devices was to create a device where the active section could be biased above threshold and the passive cavity could be used as a modulator. The devices were designed so that small changes to the passive cavity would produce large changes in the lasing output intensity. We have found that both forward bias and reverse bias current injection into the passive cavity can modulate the laser emission. We have also found that under reverse bias modulation at high speeds Q-switched pulses can be generated.

3.1. Optical Modulation

Figure 4 shows the CRVCL output intensity as a function of active cavity current for a 20 x 20 μm oxide aperture (lower cavity) at various forward bias currents supplied to a 58 x 58 μm passive cavity (upper cavity). The maximum laser intensity decreases with increasing

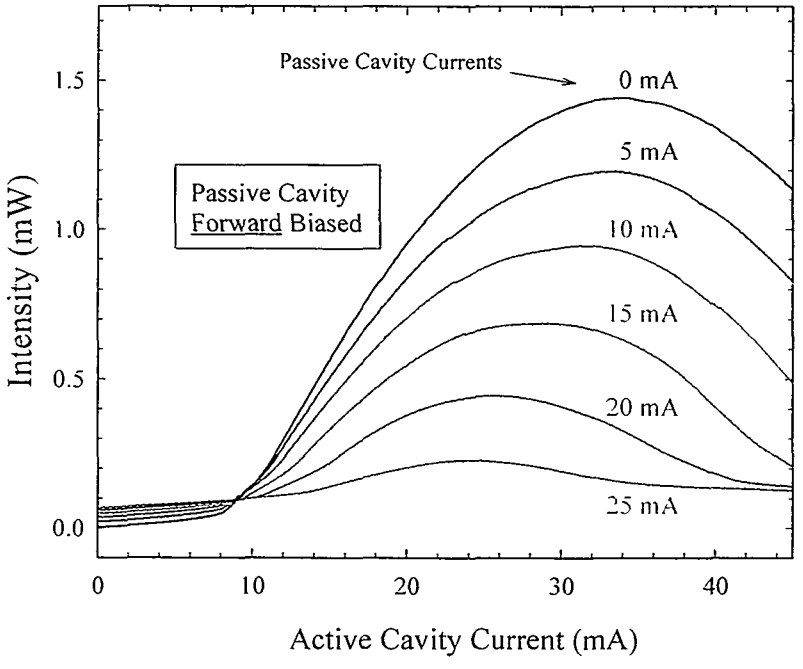

Figure 4. Light output from a CRVCL for various forward bias passive cavity currents.

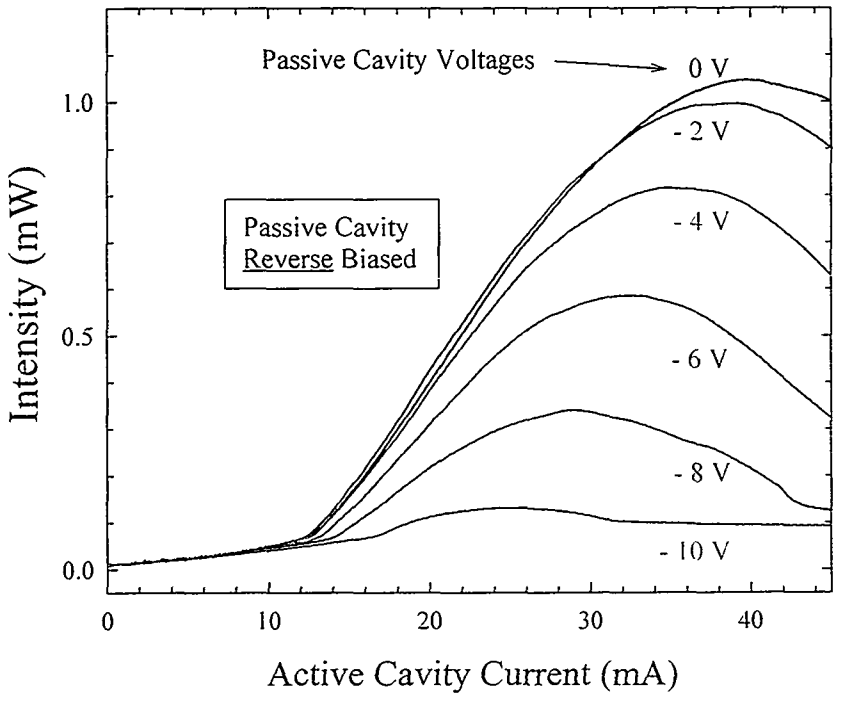

Figure 5. Light output from a CRVCL for various reverse bias passive cavity currents.

forward bias current applied to the passive cavity. As carriers are injected into the passive cavity, the index of refraction of the bulk GaAs layer is depressed causing a change in the optical path length of the passive cavity. The amount of coupling between the two cavities is changed so that a smaller fraction of the lasing mode remains in the passive cavity, which leads to a reduced output intensity. We expect that heat produced in the passive cavity will reduce the output emission, however, heating alone cannot explain the modulation observed in Fig. 4.

The output intensity of the CRVCL device can also be modulated by reverse biasing the passive cavity. Figure 5 shows the output intensity as a function of active cavity current for several different reverse bias voltages. For a given active cavity current, the output intensity decreases with increasing reverse bias voltage. Since the reverse breakdown voltage of the passive cavity diode is about – 10.5 V, considerable modulation occurs before an appreciable amount of current flows. The reverse bias modulation mechanism is therefore not related to carrier induced changes in the device but rather to the large field present in the active region. Thus, electroabsorption caused by the Franz-Keldysh effect is the most likely cause of the modulation under reverse bias conditions. Although the passive cavity is bulk GaAs, there will still be a small amount of absorption at the lasing wavelength (990 nm) induced by the applied voltage. This small amount of additional absorption is enhanced by the resonant coupling inside the cavity and can increase the loss sufficiently to drive the device below the lasing threshold.

3.2. Q-switched pulses

In addition to the device fabrication described above, the samples used to study Q-switching behavior also contained high speed probe contacts to provide efficient current injection at high frequencies. This allows the active cavity to be operated with constant current and the top cavity to be used as a modulator. Figure 6 shows a schematic of the electric field intensity inside coupled-resonator where the intensity is peaked at the GaAs absorbing layer for efficient absorption modulation.

The experiments were performed by applying a CW current just above threshold to the active cavity to generate laser emission. The passive cavity was then modulated with an RF sine wave centered around - 4 volts so that it is reverse-biased through the full period of the applied RF. Pulses were measured using a streak camera system in synchroscan mode with a 10 ps resolution. The streak camera was triggered at 80 MHz using a second, sychronized RF generator. Using this scheme, the passive cavity must always be modulated at a frequency which is an integer multiple of 80 MHz. For the frequency response measurements, an RF sweep generator connected to a scalar network analyzer was used to characterize the coupled-cavity devices.

Figure 7 shows Q-switched operation of the coupled-resonator device plotted for several different RF power levels applied to the passive cavity. The inset of the figure shows the full-width-half-maximum (FWHM) of the Q-switched pulses as a function of RF power level. The pulse width decreases with increasing RF power up to the limit of the RF generator used for these experiments. The minimum pulse width observed was 150 ps FWHM using an RF power of + 20 dBm with pulsed operation possible up to ~ 4 GHz.. The repetition rate for the data shown in Fig. 7 (and Fig. 8) was 0.88 GHz. This frequency was chosen to show the largest change in the FWHM of the pulse relative to the FWHM of the applied RF signal (570 ps @ 0.88 GHz) while still showing two pulses in the streak camera's 1.8 ns window. Thus, for the 150 ps pulse shown in Fig. 7, the pulse is compressed 3.8 times over that of the applied RF 'pulse'. The maximum achievable compression ratio was about 10.

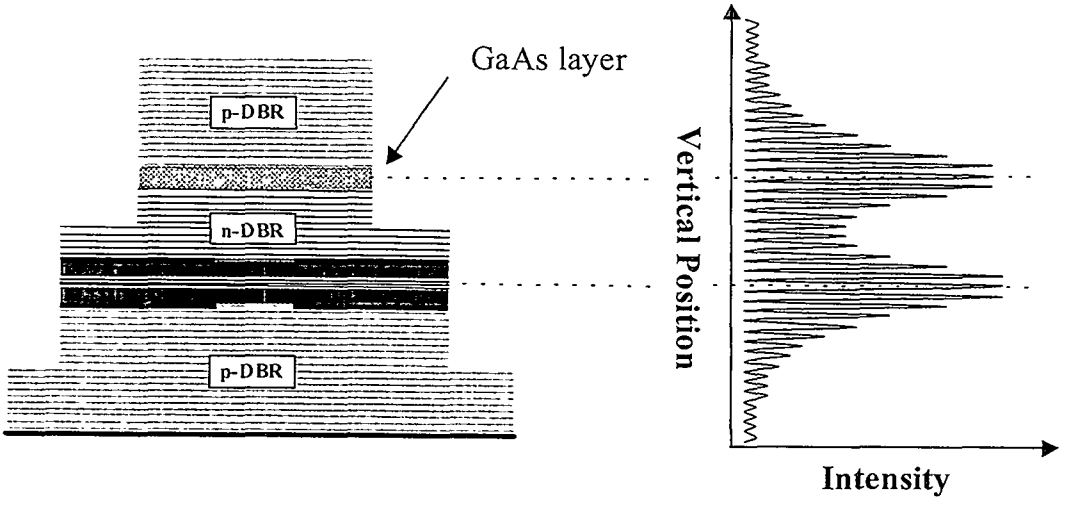

Figure 6. Schematic diagram of active-passive structure showing that the standing wave pattern is peaked in the passive cavity.

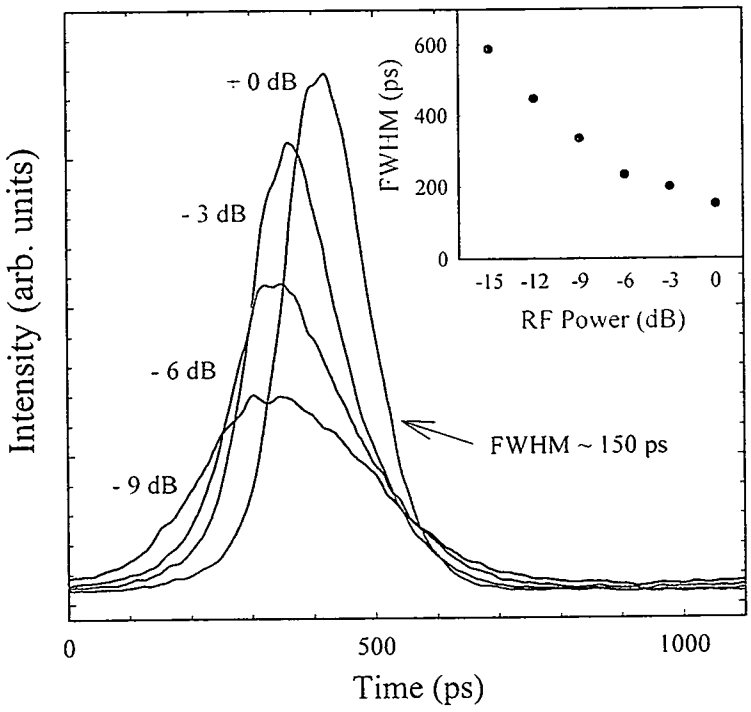

Figure 7. Q-switched pulses from a coupled-cavity plotted for several different RF power levels applied to the passive cavity. + 0 dB corresponds to + 20 dBm.

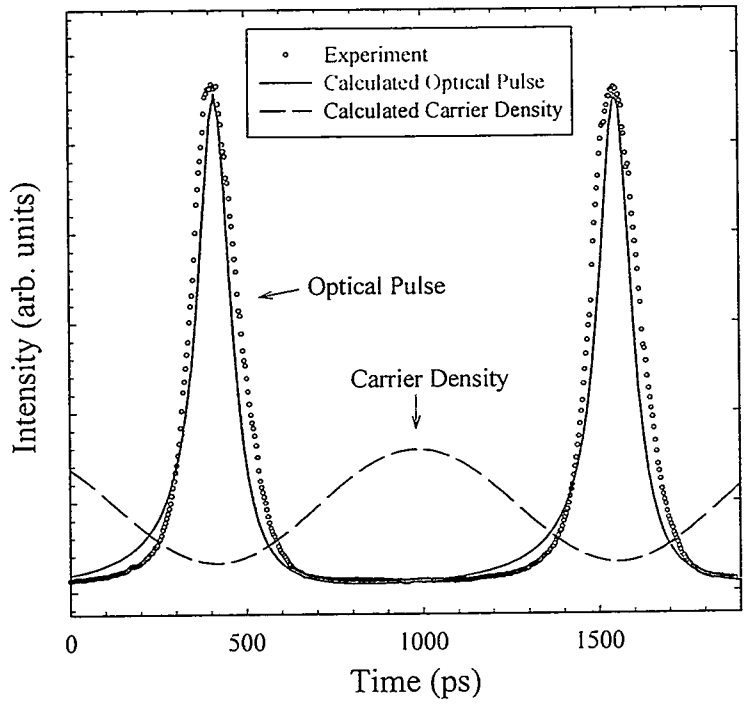

Figure 8. Calculated Q-switched pulses together with experimental data. The active cavity was supplied with a constant 14 mA, while the passive cavity was modulated at 0.88 GHz.

Under Q-switched operation, the higher power pulses appear later in time, whereas for gain-switched operation, the higher power pulses are emitted at earlier times since the gain builds up faster with stronger pumping. In these experiments, we are modulating the loss in the passive cavity while the electrical pumping to the active cavity is fixed. Pulses are emitted when the absorption in the passive cavity falls below some critical level and the cavity Q rises enough for the device to be above the lasing threshold. When higher RF powers are applied to the passive cavity, the device stays below threshold longer allowing the gain to build in the active region. When the Q of the device is restored and threshold is reduced, the emitted pulse has a higher peak power and appears at a later time. As shown in Fig. 6, the standing wave pattern in the coupled-cavity system acts to maximize the influence of the absorption in the passive cavity. In addition to this cavity enhanced absorption, the associated changes in the index of refraction in the passive cavity are large enough to cause a change in the standing wave pattern such that more (or less) of the electric field overlaps the absorbing layer. The absorption and the index will change together, but their relative importance for Q-switching is unknown. The combination of absorption and index modulation causes a change large enough to induce Q-switched operation.

Figure 8 shows a comparison between the experimental data and a simulation using the following set of rate equations:

$$\frac{dn}{dt} = \left(g - \Gamma_c - \Gamma_b \sin^2(\Omega t)\right) n \qquad (1)$$

$$\frac{dN}{dt} = P - \gamma N - gn \qquad (2)$$

where n and N are the photon and carrier densities. We approximate the modal gain by

$$g = \Gamma A \left(N - N_0\right) \qquad (3)$$

where Γ is the mode confinement factor, and, for the InGaAs QWs, we use the gain coefficient $A \approx 4.4 \times 10^{-5}$ cm^3/s and transparency carrier density $N_0 \approx 1.15 \times 10^{18}$ cm^{-3}. In the above equations, $\Gamma_c = 10^{12}$ s^{-1} is the photon decay rate in the cavity, $\Gamma_b = 1 \times 10^{13}$ s^{-1} is the amplitude of the modification of the cavity decay rate due to the reverse-bias, Ω is the modulation frequency, P is the pumping rate, and $\gamma = 10^9$ s^{-1} is the carrier decay rate. The optical pulse calculated using this rate equation approach very closely matches the experimental data in Fig. 8. The calculated carrier density shown in Fig. 8 is out of phase with the optical pulse. As expected, the carrier density increases while the cavity Q is low, and, when the cavity Q becomes high, an optical pulse is switched out of the resonator which depletes the carriers.

As shown in Fig. 9, frequency response measurements for the coupled-cavity vertical-cavity laser diode were performed at several different passive cavity bias voltages. These measurements were performed by applying a CW current to the active cavity and using the passive cavity as a modulator. A bias voltage was applied to the passive cavity together with a small-signal RF modulation. As the passive cavity diode begins to turn on (near 2 Volts), the recombination lifetime in the passive cavity limits the speed of the modulation. This can be understood as follows. Under forward-bias operation of the GaAs passive cavity, there is spontaneous emission at 870 nm, but no stimulated emission at 870 nm since the device lases at 990 nm. Because the net carrier recombination lifetime without stimulated emission is rather

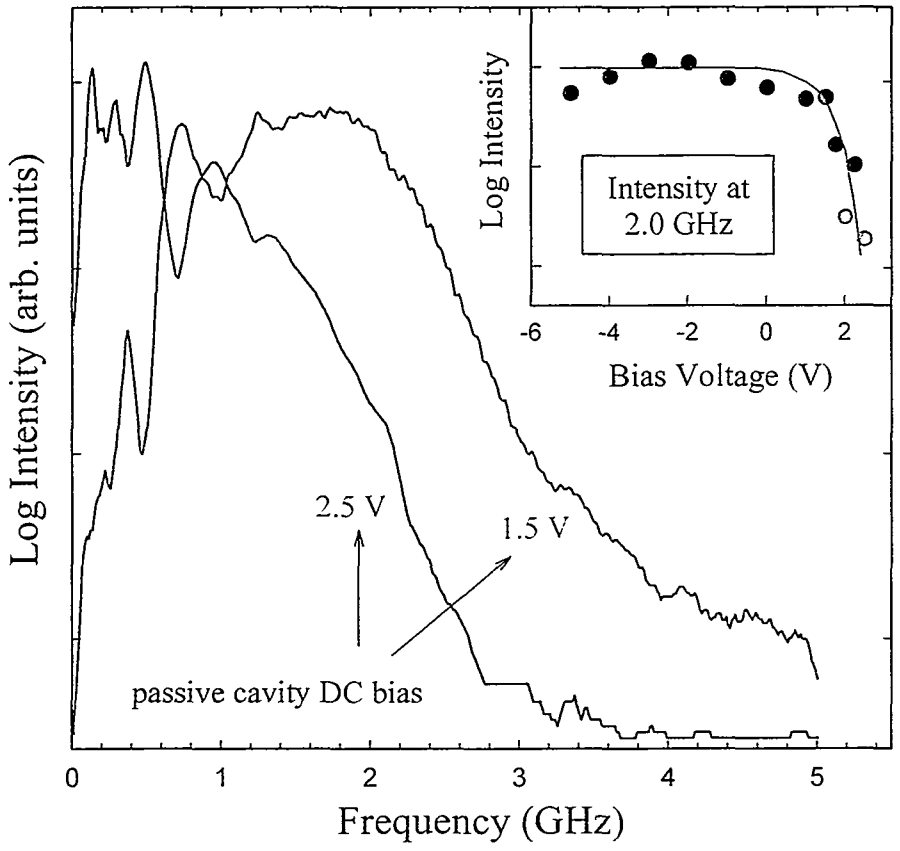

Figure 9. Frequency response data plotted for two different passive cavity bias voltages. The inset shows the intensity at 2 GHz plotted as a function of passive cavity bias voltage.

long (a few ns), the carrier density cannot be modulated at high speeds and the frequency response curve is peaked at low frequencies (~ 300 MHz). However, under reserve-bias operation there is no current flow through the passive cavity and the modulation is due only to changes in the applied field. The field can be modulated at a much higher rate which is limited by the parasitic capacitance of the device. Thus, under reverse-bias operation, the frequency response curve is peaked at higher frequencies. The transition between these two regimes occurs at about 2 volts which is the turn-on of the passive diode. The inset shows the intensity at 2 GHz modulation of the passive cavity as a function of passive cavity DC bias voltage which clearly shows a sharp drop at about 2 volts. The large size of the upper passive cavity mesa (58 x 58 μm) and the conducting substrate both contribute to device capacitance and act to limit the speed of the device.

4. Active-Active Devices

Coupled-resonator vertical-cavity lasers were also designed and fabricated with two active regions allowing us to study the interaction between the two degenerate gain regions. When both cavities have an active region, new regimes of device operation are possible. For example, we have designed CRVCL devices that lase simultaneously at both longitudinal cavity resonances. These resonances can be separated by as much as 30 nm. This dual wavelength operating regime may find applications in optical sensing and in the generation of THz frequency electric fields. We have also observed large bistability regions in the light-current curves for active-active CRVCLs. We demonstrate that this bistability can be used for high contrast optical switching using low electrical switching powers. Active-active CRVCL devices show an enhanced mode selectivity compared to single VCSEL devices. We have observed a record high 5.2 mW of power in the fundamental mode from active-active structures.

4.1. Dual Wavelength Operation

The samples designed for dual wavelength operation begin lasing at the shorter cavity resonance and as the current is increased the device will pass through a region of dual wavelength operation. At very high currents the device will only lase at the long wavelength resonance due to mismatch between the gain and the shorter cavity resonance. Figure 10 shows this progression for a constant current applied to the implant cavity and several different currents levels applied to the oxide cavity. For the data shown in Fig. 10, lasing is initiated by supplying

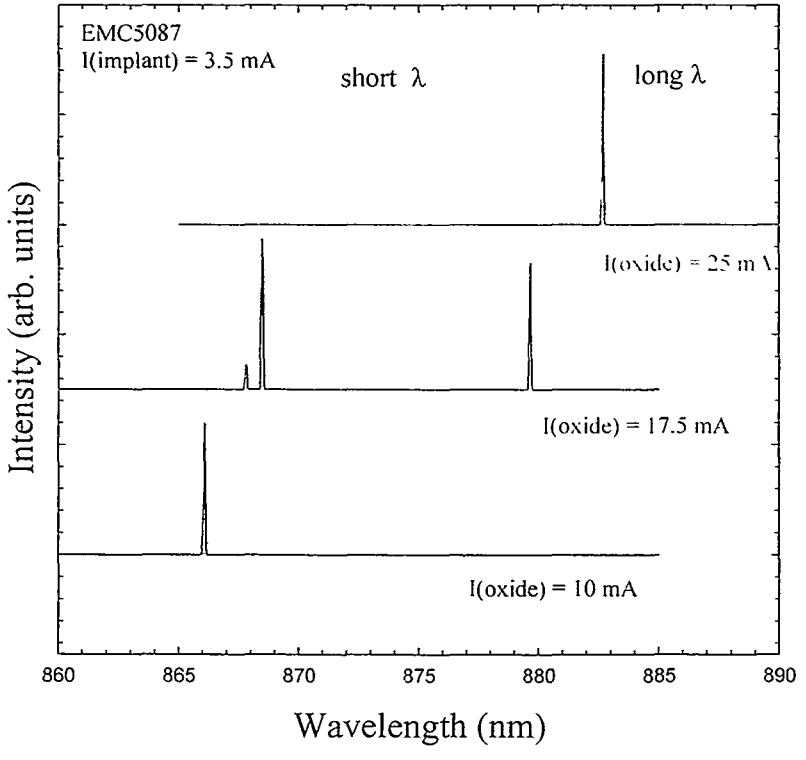

Figure 10. Lasing spectrum showing dual wavelength operation.

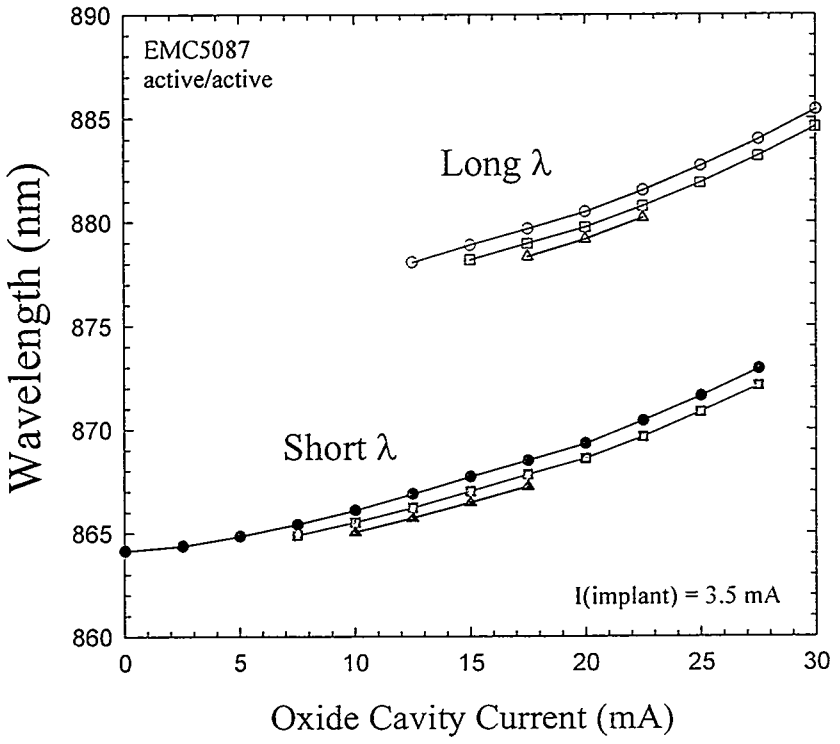

Figure 11. Lasing wavelength plotted as a function of oxide cavity current.

current to the upper, implant-defined cavity and the wavelength change is measured as a function oxide cavity current. These data are plotted in Fig. 11. There is a region near 17.5 mA where the device will lase at both longitudinal cavity resonances. The red curve is the fundamental mode while the green and black curves are higher order transverse modes. By modulating the current to one of the active regions it is possible to switch back and forth between the two wavelengths. This may be a useful device for multiwavelength optical data encoding.

4.2. Bistable Light-Current Curves

Semiconductor lasers exhibiting bistable output behavior are attractive for applications involving optical signal processing, high density optical memory, and optical interconnects. Bistable semiconductor lasers have many advantages such as low switching powers, optical gain, and high on-off state contrast. There is much interest in demonstrating bistable operation in VCSELs, which especially in the form of compact two dimensional arrays, are promising laser sources for use in optoelectronic integrated circuits. We demonstrate bistable behavior in the light-current curve of an active-active CRVCL. For comparison, devices were tested with and without the proton implant in the upper cavity . An important application for these devices is in the area of optical data encoding where the bistability leads to high contrast switching at very

low electrical switching powers. The bistability regions reported here are also much larger than with other laser structures and are positioned at the peak of the lasing output power.

Figure 12 shows bistable operation for several different bias currents applied to the top cavity. The output power is greater than 7 mW and the bistability region extends for more than 18 mA in current. This device is able to overcome the absorption in the top cavity active region and lase with no applied bias current. With increasing bias current to the top cavity, the bistability window decreases in size and shifts to higher currents. The lasing threshold decreases and the output power increases with increasing top cavity bias. At very large biases applied to the top cavity, the bistability region becomes very small and in some cases disappears. These observations are consistent with a lowering of the absorption in the top cavity as the bias is increased. The size and position of the bistability region was observed to vary for devices at different locations across the wafer.

One of the most interesting features of this data is the abrupt shut-off observed at high oxide cavity currents. A VCSEL typically shows a smooth thermal shut off due to a misalignment of the gain and the cavity resonance at higher temperatures. Since the device abruptly transitions from multimode lasing to below threshold luminescence, polarization or transverse mode hopping can be ruled out as the mechanism. We believe that the abrupt shut-off in the CRVCL is due to the combination of saturable absorption in the top cavity and thermal rollover in the bottom cavity. This mechanism is supported by the observation that the devices generally do not shut off until they are at or near the thermal rollover point on the light-current curve.

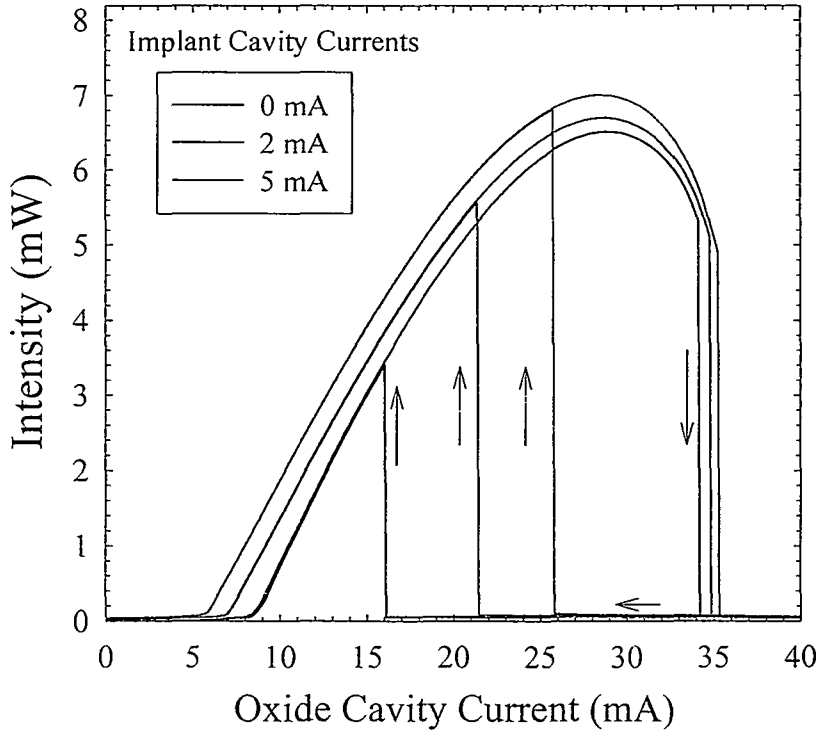

Figure 12. Bistable light vs. current curve plotted for three different top cavity bias currents.

To model the experiment, we assume that the bottom cavity operates as a laser, with a typical light-current curve of a VCSEL. We treat the response of the top cavity to the injection of laser light from the bottom cavity according to the theory of Spencer and Lamb [9]. Solution of the Spencer and Lamb equations for a given injected laser field can lead to single-stable or bistable steady-state solutions, depending on the combination of injected intensity, nonlinear absorption in the top cavity, and detuning between the two cavities. The changes in these quantities are assumed to arise from heating. Figure 13 shows the calculated output intensity from the top cavity together with the experimental data. The calculation qualitatively reproduces the experimental data with the bistability observed near the peak of the laser emission. The calculation suggests that the bistability is caused by the saturable absorption in the top cavity combined with the heating effects near the thermal rollover point of the bottom cavity.

It is also possible to use a coupled-resonator vertical-cavity laser as a high contrast switching device. Through small changes in the top cavity bias current it is possible to switch between lasing at ~ 4 mW to subthreshold lasing at 40 μW. Fig. 14a shows the light-current curve for two different bias currents for a device with an air-post top cavity. Fig. 14b shows the corresponding emission spectrum on a log scale with the oxide cavity current fixed at 31.5 mA. The top curve shows the multimode lasing spectrum at the longer cavity resonance for a 3.5 mA top cavity bias and the bottom curve shows emission at 2.5 mA bias where two broad subthreshold luminescence peaks are observed at the long and short cavity resonances. Thus, it is possible to switch the device on and off by varying the bias current to the top cavity by as little as 1 mA. Similar data can be obtained for a device with an implanted top cavity (not shown). Since the implant aperture creates a higher current density for a given input current, the device can be turned off and on by changing the top cavity bias by as little as 0.1 mA. Thus, changes in electrical power as low as 250 μW can change the output state intensity by two orders of magnitude. Further experiments are required to determine if the coupled-resonator vertical cavity laser can be switched using external optical injection.

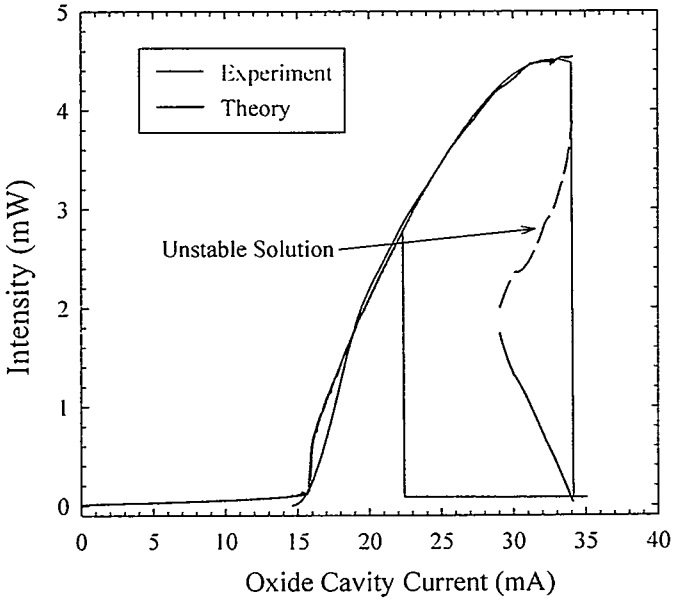

Figure 13. Calculated bistable light vs. current curve together with experimental data.

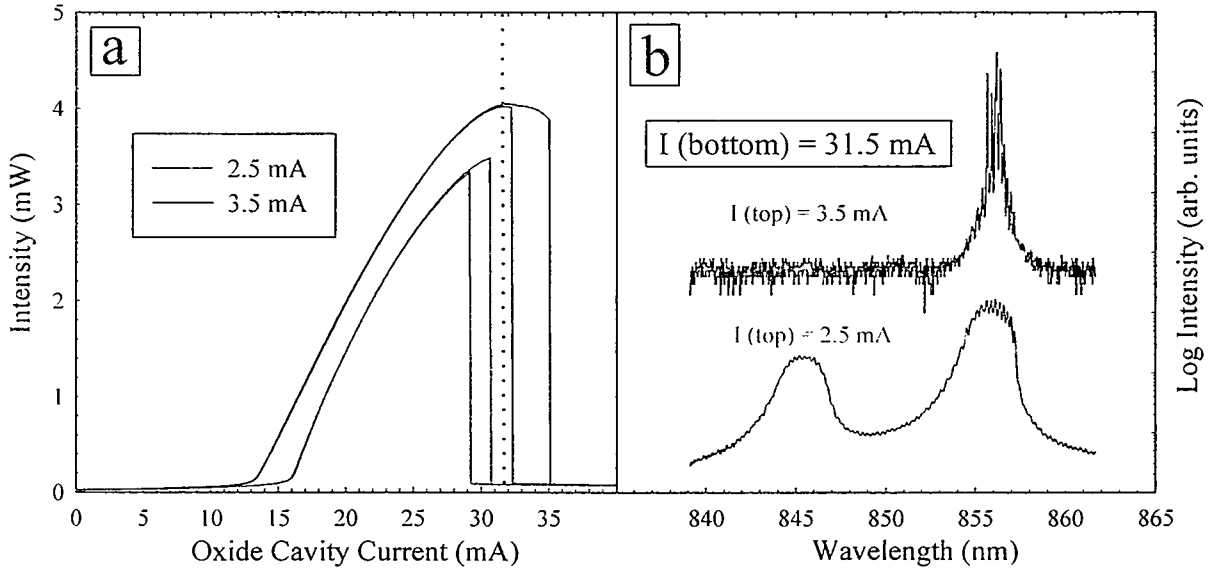

Figure 14. (a) light vs. current curves for two different implant cavity bias currents. (b) Emission spectra at an oxide cavity current of 31.5 mA. Note the transition from multimode lasing at the long wavelength resonance to subthreshold luminescence from both cavity resonances.

4.3 Single-Mode Operation

High power single-mode operation is essential for many applications including laser printing, optical storage, efficient coupling to single-mode fibers, and optical sensing. We have achieved a record high single-mode power of 5.2 mW from our CRVCL devices which is possible due to the coupled-resonator geometry. In conventional vertical-cavity surface-emitting lasers, the extent to which the gain volume may be increased is limited by the onset of multimode operation. Our results show that this limitation is circumvented in a coupled-resonator device allowing very high single-mode operation.

Figure 15a shows the lasing spectrum of a CRVCL device with 13.7 mA applied to the oxide cavity and 5.0 ma applied to the implant cavity. The main lasing peak is at 853.8 nm and the next largest higher-order mode is 32 dB lower. Figure 15b shows a light current curve for the same device at the same implant cavity current of 5.0 mA. At the dashed line, which denotes an oxide cavity current of 13.7 mA, the device is lasing single-mode with an output power of 5.2 mW.

Although we have observed record high single-mode output powers from a CRVCL device, in order to be useful for many applications, the single-mode must also be the lowest order fundamental Gaussian mode. In order to determine if the single mode that we are observing is the fundamental mode, we measured the lasing wavelength for all detectable modes as a function of oxide cavity current under the conditions where single-mode operation is observed. Figure 16

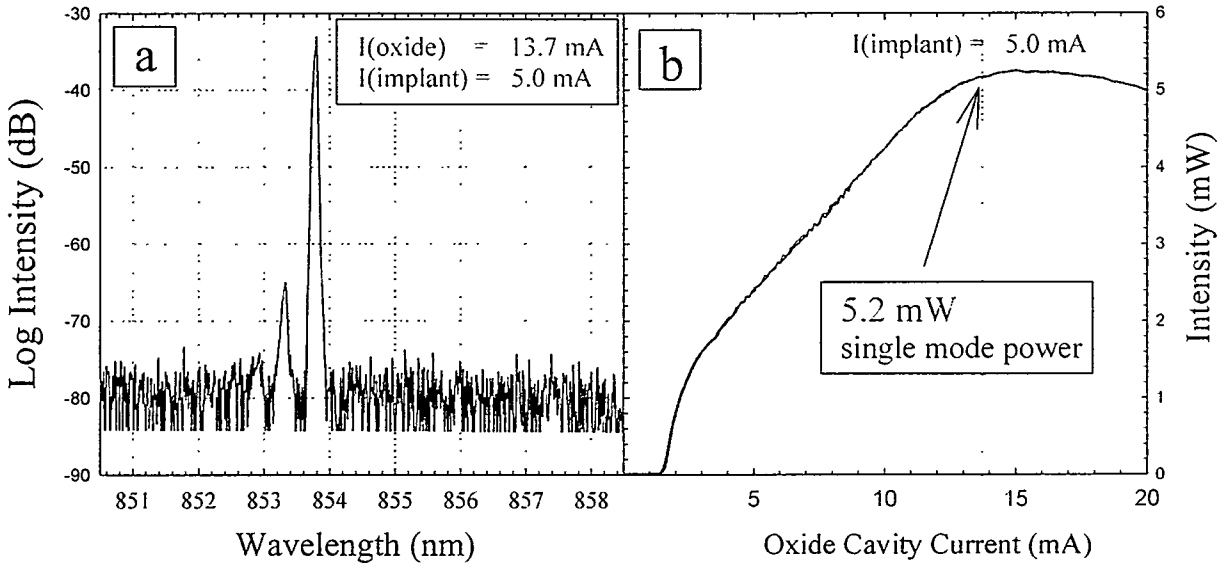

Figure 15. (a) Lasing spectrum taken with I(oxide) = 13.7 mA and I(implant) = 5.0 mA. (b) Light-current curve with the implant cavity current at 5.0 mA showing 5.2 mW of single-mode power.

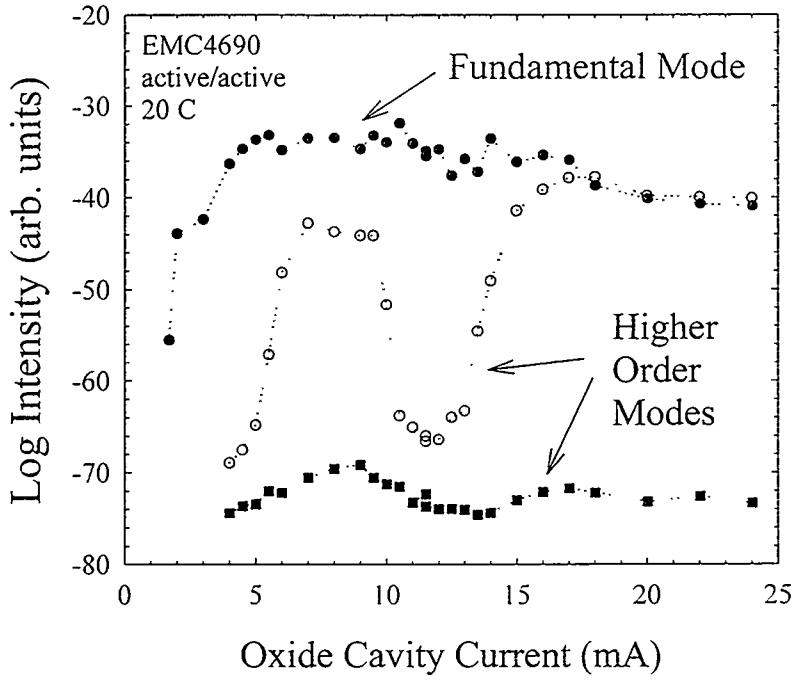

Figure 16. (a) Emission wavelength plotted as a function of oxide cavity current for all observable cavity modes.

shows the relative lasing intensity for three cavity modes. The device begins lasing on the long wavelength side. As the oxide cavity current is increased, two additional modes are observed on the high energy side. It is known that higher order modes in a VCSEL will always be at higher energy than the fundamental mode. Since oxide-confined VCSELs typically begin lasing on the fundamental mode, we know our devices are lasing on the lowest order fundamental Gaussian mode.

4. Summary

We have designed and fabricated electrically-injected coupled-resonator vertical-cavity lasers and have studied the novel properties of both active-passive and active-active devices. The active-passive structure was designed to be used as a modulator. The laser intensity can be modulated by either forward or reverse biasing the passive cavity. Under forward bias operation of the passive cavity, the modulation arises from dynamic changes in the coupling between the active and passive cavities. Under reverse bias operation, the modulation is caused by the Franz-Keldysh effect in the passive cavity. Furthermore, under reverse bias operation, Q-switched pulses have been observed. The Q-switched operation is possible in this structure due to cavity coupling which allows large changes in the cavity Q with only very small changes in absorption. Q-switched pulses as short as 150 ps have been observed and at repetition rates as high as 4 GHz. A rate equation approach is used to model the Q-switched operation yielding good agreement between the experimental and theoretical pulseshape.

We have designed and demonstrated the operation of active-active devices which lase simultaneously at both longitudinal cavity resonances. Extremely large bistable regions have also been observed in the light-current curves for active-active coupled resonator devices. This bistability can be used for high contrast switching with contrast ratios as high as 100:1. Coupled-resonator vertical-cavity lasers have shown enhanced mode selectivity which has allowed devices to lase with fundamental-mode output powers as high as 5.2 mW. The new operating regimes discovered using multiple-section vertical-cavity lasers, such as bistable operation and high single-mode power, will enable many emerging VCSEL applications in telecommunications, high-speed data encoding, and optoelectronic interconnects.

References

[1] W.T. Tsang, in *Semiconductors and Semimetals; Vol. 22 B,* edited by R.K.Willardson and A.C. Beer (Academic, New York, 1985), p.257.

[2] W.W. Chow, IEEE J. Quantum Electron. **QE-22**, 1174 (1986).

[3] K.D. Choquette, W.W. Chow, H.Q. Hou, K.M. Geib, and B.E. Hammons, Proceeding of the SPIE-The International Society for Optical Engineering **3286,** 134 (1998).

[4] A.J. Fischer, K.D. Choquette, W.W. Chow, H.Q. Hou, and K.M. Geib, "Coupled-Resonator Vertical-Cavity Laser Diode," Appl. Phys. Lett. **75,** 3020 (1999).

[5] A.J. Fischer, W.W. Chow, K.D. Choquette, A.A. Allerman, and K.M. Geib, "Q-switched Operation of a Coupled-Resonator Vertical-Cavity Laser Diode," Appl. Phys. Lett. **76,** 1975 (2000).

[6] A.J. Fischer, K.D. Choquette, W.W. Chow, A.A. Allerman, and K.M. Geib, "Record High Single-Mode Power from a Coupled-Resonator Vertical-Cavity Laser," (to be published).

[7] P. Michler, M. Hilpert, and G. Reiner, Appl. Phys. Lett. **70,** 2073 (1997).

[8] R.P. Stanley, R.Houdré, U.Oesterle, M. Ilegems, and C. Weisbuch, Appl. Phys. Lett. **65,** 2093 (1994).

[9] M.B. Spencer and W.E. Lamb, Jr., Phys. Rev. A **5,** 884 (1972).

Appendix A: Sandia CRVCL publications and presentations

Publications

K.D. Choquette, W.W. Chow, H.Q. Hou, K.M. Geib, and B.E. Hammons, "Coupled-Resonator Vertical-Cavity Laser Diode," Proceeding of the SPIE- The International Society for Optical Engineering **3286,** 134 (1998).

A.J. Fischer, K.D. Choquette, W.W. Chow, H.Q. Hou, and K.M. Geib, "Coupled-Resonator Vertical-Cavity Laser Diode," Appl. Phys. Lett. **75,** 3020 (1999).

A.J. Fischer, W.W. Chow, K.D. Choquette, A.A. Allerman, and K.M. Geib, "Q-switched Operation of a Coupled-Resonator Vertical-Cavity Laser Diode," Appl. Phys. Lett. **76,** 1975 (2000).

A.J. Fischer, K.D. Choquette, W.W. Chow, A.A. Allerman, and K.M. Geib, "Bistable Output from a Coupled-Resonator Vertical-Cavity Laser Diode," (to be published).

A.J. Fischer, K.D. Choquette, W.W. Chow, A.A. Allerman, and K.M. Geib, "Record High Single-Mode Power from a Coupled-Resonator Vertical-Cavity Laser," (to be published).

Presentations

"Coupled-Resonator Vertical-Cavity Laser Diodes," 1999 LEOS summer topical, VCSELs and Microcavitites, San Diego, CA - (invited talk).

"Q-switched Operation of a Coupled-Resonator Vertical-Cavity Laser Diode," 1999 LEOS Annual Meeting, San Fransisco, CA - (post deadline paper).

"Bistable Operation of a Coupled-Resonator Vertical-Cavity Laser Diode," 2000 CLEO conference, San Fransisco, CA - (contributed talk).

Sandia is a multiprogram laboratory operated by Sandia Corporation, a Lockheed Martin Company, for the United States Department of Energy under Contract DE-AC04-94AL85000.

15	MS-0603	Arthur Fischer (1742)
1	MS-9018	Central Technical Files (8940-2)
2	MS-0809	Technical Library (9612)
1	MS-0619	Review and Approval Desk (9612)
1	MS-0188	LDRD Office (4001)